

Large-Area Single-Mode VCSELs and the Self-Aligned Surface Relief

Heiko J. Unold

The effect of mode-profile specific etching of the top layer in selectively oxidized VCSEL structures at 850 nm emission wavelength is examined. For high reproducibility, a self-aligned etching technique is used which aligns surface etch and oxide aperture by only one additional photoresist step. By optimizing layer structure and etch spot size, completely single-mode devices with aperture diameters up to 16 μm are obtained. Maximum single-fundamental mode output power of 3.4 mW at room temperature and over 4 mW at 0°C is obtained with a maximum far-field angle of 5.5°. Using parameters for etch spot height and diameter, Gaussian beam spot size and phase curvature, the measured diffracted far-field distribution is fitted well over a 20 dB intensity range. The chosen fit parameters therefore enable to estimate the amount of phase curvature within the VCSEL for different operation currents, which cannot be obtained with available measurement methods.

1. Introduction

High power single-mode emission from vertical cavity surface-emitting lasers (VCSELs) is currently considered a main challenge in opening up new application fields for these promising devices. Their vertical layer structure, apart from significantly facilitating production and testing, also enables integration of one- and two-dimensional arrays which can be used conveniently in parallel data transmission or to obtain cumulative high output power. Due to the very short cavity, longitudinal single-mode operation is inherent to the VCSEL structure. Small oxide aperture VCSELs below about 4 μm diameter also operate in the fundamental transverse mode. Unfortunately, the rather large differential resistance and high current densities in these small devices can affect lifetime. When the aperture diameter is increased to obtain higher output power, however, multiple higher-order transverse modes oscillate, causing increased noise, a much broadened spectrum, and a strong increase of the far-field angle. More specifically, since the number of transverse modes oscillating depends on pumping profile and thermal conditions, these values are subject to strong variations with current, thus rendering optical properties of the VCSEL unreliable. Previous attempts in increasing single-mode output power include external reflectors and other optical elements, increasing the cavity length [1, 2], hybrid implant/oxide VCSELs [3], metal apertures [4], and surface etching [5, 6, 7, 8]. We present the application of an optimized self-aligned shallow surface etch to force oxidized VCSELs of up to 16 μm aperture diameter to operate on the fundamental mode from threshold to

thermal roll-over. Increasing the active diameter while maintaining single-mode emission promises low series resistance, long lifetime and high single-mode output power at small divergence angles.

2. Device Structure and Processing

As described previously, our self-aligned surface etching process allows to align the surface relief automatically to the oxide aperture respective mesa with high precision by only one additional photoresist step [8]. Fig.1 displays a top view photograph along with a schematic cross-section of a finished device. By simulating the threshold gain of the structure and successively removing part of the top mirror, we can determine the optimum etch depth for any given structure. For simulation, a one-dimensional transfer matrix program is used. As can be expected, due to the periodic nature of a phase variation, the result is a periodic increase and decrease of the threshold gain. When a layer of about $\lambda/2$ thickness has been removed, the threshold gain reaches a minimum, essentially showing the behavior of a VCSEL structure with one Bragg pair less. At the anti-resonance thickness in between, at about $\lambda/4$, a rather narrow local maximum is observed. With our wet chemical etch process, a precision of about ± 3 nm can be reached, which is sufficient to achieve a strong effect but cannot guarantee maximum threshold gain contrast. The epitaxial structure of the examined sample consists of a 20-pair C-doped p-DBR, three 8 nm quantum wells between 10 nm $\text{Al}_{0.28}\text{Ga}_{0.72}\text{As}$ barriers, and a 37.5-pair Si-doped n-DBR, leading to an optimum surface etch depth of about 58 nm.

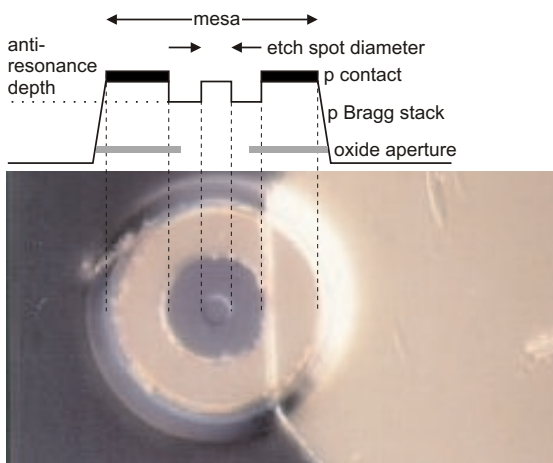


Fig. 1. Top-view photograph and schematic cross-section of the VCSEL structure. In the center the $5\ \mu\text{m}$ diameter etch spot can be seen, surrounded by the anti-resonant DBR region.

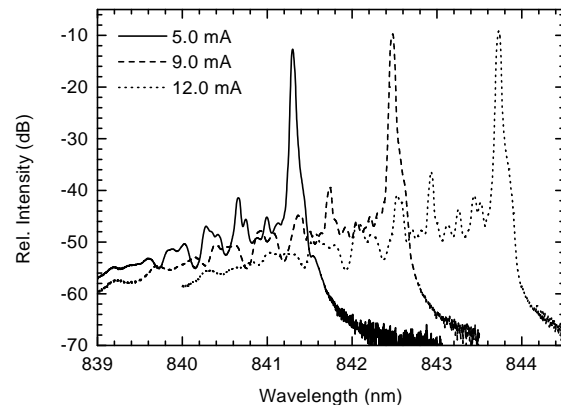


Fig. 2. Spectra measurements for currents from threshold to roll-over for the $11\ \mu\text{m}$ aperture device with $5\ \mu\text{m}$ etch spot diameter.

3. Output Characteristics

As opposed to previous samples, where surface etching only introduced a certain limited single-mode operation range to devices of up to $7\ \mu\text{m}$ diameter [8], the improved layer structure and processing have much augmented the effect. The comparison of unetched devices and etch spots of 3 and $5\ \mu\text{m}$ diameter on $11\ \mu\text{m}$ oxide aperture VCSELs in Fig. 3 confirms that surface etching can have a large impact on laser operation. However, even though threshold is increased and maximum output power is decreased, the fact that the shape of the L-I curves remains smooth is important e.g. for data transmission applications. As shown by the spectra measurements in Fig. 2, although many modes exist, etched devices remain completely single-mode with more than 30 dB SMSR up to thermal roll-over. This indicates that while single-mode operation can be forced upon devices of virtually any size using a small enough etch diameter, an optimum etch diameter exists where single-mode output power is maximum. The oxide aperture size dependence for a

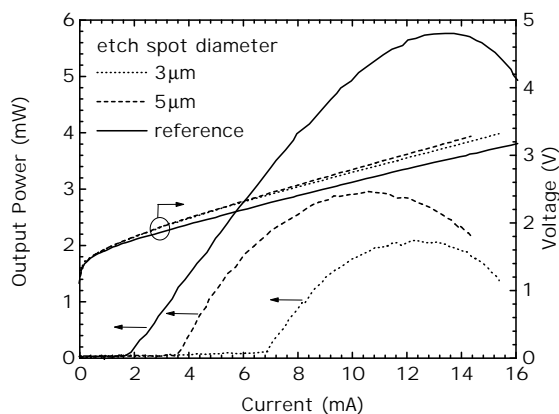


Fig. 3. LIV characteristics of $11\ \mu\text{m}$ diameter devices with different etch spot diameters.

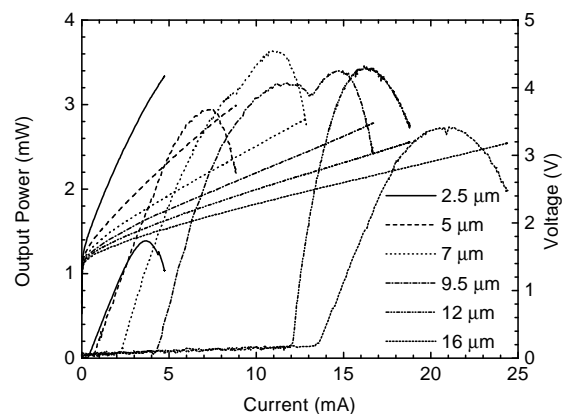


Fig. 4. LIV characteristics of devices with $5\ \mu\text{m}$ etch spot having various aperture diameters.

fixed etch spot diameter of $5\ \mu\text{m}$ is illustrated in Fig. 4. Small devices up to $7\ \mu\text{m}$ aperture diameter exhibit threshold and power scaling as would be observed on standard devices, showing that an etch spot of this size does not influence these devices significantly. For the 12 and $16\ \mu\text{m}$ devices, however, threshold is increased drastically and maximum power even decreases slightly. Since these devices are single-mode, this behavior is consistent with the above discussion on etch spot size dependence. The sudden increase in threshold for the large single-mode devices is caused by a large carrier leakage in the outer regions where no lasing occurs. The $9.5\ \mu\text{m}$ device represents the transition size: having reasonable threshold, thermal roll-over occurs rather early and with less power than the $7\ \mu\text{m}$ device. The device is already forced to the fundamental mode up to this point. For the second local maximum, however, a second mode of comparable intensity is observed. One last interesting feature is the extremely high differential quantum efficiency of the $12\ \mu\text{m}$ device of close to 100%, indicating a continuous improvement of the overlap between the

fundamental mode and the small high reflective region by increased thermal guiding as current is increased. These results therefore confirm that a maximum etch spot size exists for single-mode emission for any given aperture diameter. Additionally, they imply that a certain thermal gradient is also necessary in the VCSEL to force operation on the fundamental transverse mode, illustrated by the high differential quantum efficiency of the $12\ \mu\text{m}$ device and the rather large wavelength shift with current for devices of this size.

4. Far-Field Measurements and Fit Function

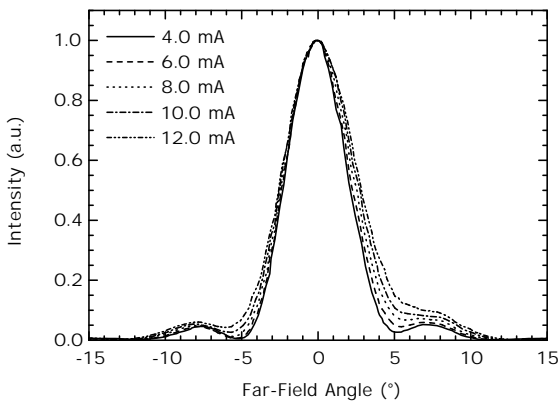


Fig. 5. Far-field measurements for currents from threshold to roll-over for the $11\ \mu\text{m}$ oxide aperture, $5\ \mu\text{m}$ etch spot device.

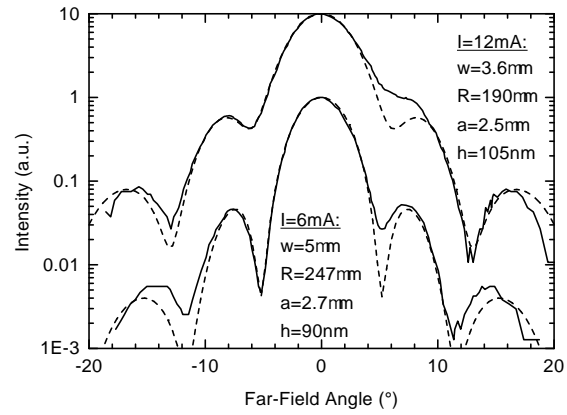


Fig. 6. Logarithmic plot of near-field fit function transformed to far-field (dashed lines) with corresponding far-field measurements (solid lines) for currents of 6 and 12 mA.

The far-field measurements on the $11\ \mu\text{m}$ oxide aperture device with $5\ \mu\text{m}$ etch spot diameter shown in Fig. 5 again confirm single-mode emission by the small full-width half-maximum (FWHM) far-field angle of 4.3° which only broadens by about 20% over the whole operating range. The far-field angle of the corresponding reference device increases from 5.3° to 11° already at two times threshold. However, the stable side lobes in the far-field of the etched device indicate that diffraction already takes place at the surface etch. In order to investigate the origin of the diffraction pattern, we have adopted a model which fits a Fourier-transformed calculated near-field distribution to the measured far-field data. The near-field function is assumed to be a Gaussian profile with spot size ω and phase curvature R

$$E(r) = u(r) \cdot \hat{E} \cdot \exp \left\{ - \left(\frac{r^2}{\omega^2} + i \frac{\pi \bar{n} r^2}{\lambda R} \right) \right\}, \quad (1)$$

where the phase is locally delayed by the difference in optical lengths between etched and unetched regions expressed by

$$u(r) = \exp \left\{ i \text{rect} \left(\frac{r}{a} \right) \left[\frac{2\pi h}{\lambda} (\bar{n}_0 - \bar{n}) \right] \right\}. \quad (2)$$

Here, r is the radial coordinate, a describes etch spot radius, h etch depth, \bar{n} and \bar{n}_0 refractive indices in GaAs and air, respectively, and λ the vacuum wavelength. The resulting far-field fit curves are plotted logarithmically for two currents around threshold and at roll-over along with the corresponding measured data in Fig. 6. The good agreement over 20 dB in intensity confirms the validity of the model, especially the choice of fitting parameters. More specifically, the measured data, namely the radial position of the minima, cannot be fitted sufficiently without assuming a curved wavefront in the Gaussian near-field. The geometric parameters a and h can be measured directly and ω is obtained by near-field measurements. We can therefore, to our knowledge for the first time, estimate the phase curvature of the Gaussian beam within an experimental VCSEL by a simple fit to measured data. The obtained values range from 190 to 250 μm for a 11 μm aperture device depending on pumping current. It can therefore be concluded that thermal guiding influences the phase curvature strongly, i. e. it significantly contributes to guiding in these weakly index guided devices having a thin oxide aperture in a standing wave pattern node.

5. Conclusion

We have investigated oxidized VCSELs with self-aligned circular surface etch patterns between 3 and 10 μm diameter having aperture diameters between 2.5 and 16 μm . Single-fundamental mode emission with a side-mode suppression ratio of 30 dB is obtained from threshold to thermal roll-over for all device sizes with appropriate etch spot diameters. 12 μm -aperture devices with 5 μm etch spot diameter achieve 3.4 mW single-mode output power at room temperature and more than 4 mW at 0°C. Due to diffraction at the surface etch, the FWHM far-field angle is stabilized to below 5.5°. Comparison of the different device sizes, pulsed and cooled measurements lead us to the conclusion that increased guiding could significantly reduce threshold and thus enhance single-mode power output. A further increase in single-mode power is expected from additionally restricting the gain laterally to match the surface etch spot.

References

- [1] D. G. Deppe and D. L. Huffaker, “High spatial coherence vertical-cavity surface-emitting laser using a long monolithic cavity”, *Electron. Lett.*, vol. 33, pp. 211–213, 1997.
- [2] H. J. Unold, S. W. Z. Mahmoud, R. Jäger, M. Kicherer, M. C. Riedl, and K. J. Ebeling, “Improving Single-Mode VCSEL Performance by Introducing a Long Monolithic Cavity”, *Photon. Techn. Lett.*, vol. 12, pp. 939–941, 2000.
- [3] K. D. Choquette, A. J. Fischer, K. M. Geib, G. R. Hadley, A. A. Allerman, and J. J. Hindi, “High Single Mode Operation from Hybrid Ion Implanted/Selectively Oxi-

- dized VCSELs”, in *Proc. IEEE 17th International Semiconductor Laser Conference*, Monterey, U.S.A., Sept. 2000, pp. 59–60.
- [4] T. Nakamura, H. Nakayama, A. Sakamoto, N. Ueki, J. Sakurai, H. Otoma, Y. Miyamoto, and M. Fuse, “High Power Single-Mode 780 nm Oxide-Confined VCSEL with Metal Aperture as a Spatial Filter”, in *Proc. IEEE 16th International Semiconductor Laser Conference*, Nara, Japan, Oct. 1998, pp. 7–8.
- [5] P. Dowd, L. Raddatz, Y. Sumaila, M. Asghari, I. H. White, R. V. Penty, P. J. Heard, G. C. Allen, R. P. Schneider, M. R. T. Tan, and S. Y. Wang, “Mode Control in Vertical-Cavity Surface-Emitting Lasers by Post-Processing Using Focused Ion-Beam Etching”, *Photon. Techn. Lett.*, vol. 9, pp. 1193–1195, 1997.
- [6] L. M. A. Plouzenec, L. J. Sargent, R. V. Penty, and I. H. White, “Gaussian Beam Profile and Single Transverse Mode Emission from Previously Multi-Mode Gain Guided VCSEL using Novel Etch”, in *Vertical-Cavity Surface-Emitting Lasers IV*, C. Lei K. D. Choquette, Ed., Proc. SPIE, 2000, vol. 3946, pp. 219–229.
- [7] H. Martinsson, J. A. Vukušić, and A. Larsson, “Single-Mode Power Dependence on Surface Relief Size for Mode-Stabilized Oxide-Confined Vertical-Cavity Surface-Emitting Lasers”, *Photon. Techn. Lett.*, vol. 12, pp. 1129–1131, 2000.
- [8] H. J. Unold, M. Grabherr, F. Eberhard, F. Mederer, R. Jäger, M. Riedl, and K. J. Ebeling, “Increased-area oxidised single-fundamental mode VCSEL with self-aligned shallow etched surface relief”, *Electron. Lett.*, vol. 35, pp. 1340–1341, 1999.